An Evaluation of Non-Stochastic Lattice Structures Fabricated Via Electron Beam Melting.

O. Cansizoglu, D. Cormier, O. Harrysson, H. West, and T. Mahale
North Carolina State University
Edward P. Fitts Department of Industrial and Systems Engineering
Raleigh, NC 27695-7906

Abstract

Metal foam structures have many applications and can be used as structural supports, heat exchangers, shock absorbers, and implant materials. Stochastic metal foams having different cell sizes and densities have been commercially available for a number of years. This paper addresses a different type of foams which are known as non-stochastic foams, or lattice structures. These foams have a well defined repeating unit cell structure rather than the random cell structure in commercially available stochastic foams. The paper reports on preliminary research on the fabrication of non-stochastic Ti-6Al-4V alloy foams using the Electron Beam Melting process. Behavior of the structures in compression, bending, and low cycle repeating load tests are discussed, and recommendations about cell geometry and processing conditions are made.

Introduction

Stochastic metal foams have been commercially available for some time, and are used in a wide variety of applications. These foams can have either open or closed cell structures. Closed cell foams are typically produced by adding gas directly to melt, adding gas releasing blowing agents or causing precipitation of gas bubbles (Banhard, 2000). The process is controlled to achieve the desired pore size, pore shape, and pore distributions, which in turn influence the material properties (see Brothers and Dunand, 2006). Combustion synthesis has also been used to produce metallic foams. Reactants are mixed, cold pressed and placed in an inert atmosphere and ignited to start the thermal explosion mode or self-propagating high thermal synthesis. Zhang et al. (2001) used combustion synthesis to produce porous surfaces having bone ingrowths without immune response. Powder metallurgy (PM) is a common technique to produce cellular structures where porosity is a natural result of the process. Porosity levels may also be increased by adding blowing agents. The powder mixture is compacted to get a semi finished product. This is followed by heat treatment at near melting temperature of the matrix material. The blowing agent releases gas during the heat treatment. These methods are suitable for Al, Zn, and Mg foams, however Ti is unsuitable due to its high melting temperature and reactivity. Conventional sintering of titanium alloy powders requires sustained high temperature and vacuum. Wen et al. (2002) fabricated titanium foams using PM including space holder particles where the resulting densities varied from 50% to 65%. Baumeister et al. (1997) used PM to manufacture aluminum foams. Metallic powders were mixed with foaming agents and compacted to semi finished products. Li et al. (2006) used polyurethane struts produced through RP as a mold and coated them with titanium (Ti-6Al-4V) slurry. After the polyurethane was burned off, the powder was sintered resulting in a porous titanium structure with a porosity of 88% and a compressive strength of 10 MPa. Medlin et al. (2004) report on a method for making tantalum Trabecular Metal®. Carbon skeletons are first obtained by pyrolizing thermosetting polymer foams with repeating dodecahedron structure. Pore size and density of the original polyurethane foam affects

the pore size and mechanical properties of the Trabecular Metal®. A 50μm tantalum film is then deposited onto this carbon skeleton via chemical vapor deposition with a 50μm coating thickness. This process results in a favorable microstructure resulting from proper orientation during deposition and crystallographic growth. Trabecular Metal® has been reported to have superior mechanical properties with an elastic modulus of 3Gpa. Wadley et al. (2003) discussed manufacturing methods of periodic cellular metals. Metallic sandwich panels with periodic open cell cores were found to possess better load sustaining capabilities than stochastic foams.

Figure 1 Stochastic Copper Foam

SFF processes have also been used to fabricate repeating mesh structures. 3D mesh structures in stainless steel and cobalt-chrome were built with Selective Laser Melting (SLM) technology and resulted in nearly 90% reduction in weight (www.mcpgroup.com).

The remainder of this paper describes the testing and evaluation of non-stochastic lattice structures produced via the Electron Beam Melting (EBM) process. There were several objectives associated with this preliminary research. The first was to experiment with process settings needed to fabricate these mesh structures. The second was to determine limits on the achievable feature sizes and cell densities. A third objective was to select one cell geometry and gather preliminary material properties.

Experimental Procedure

Preliminary experimentation started with determining process settings that would produce reasonably cohesive cellular structures. As the objective to this point has been to study the bounds of what can feasibly be made via the EBM process, no attempt has yet been made to optimize the process settings. Starting with initial settings suggested by Arcam, experimentation led to the following melting procedure for lattices. The entire powder bed is first scanned 20 times at 10,000 mm/sec with the beam power gradually ramping up from 6W on the first scan to 1200W on the final scan. The lattice geometry for a given layer is then melted at 180 mm/sec with a beam power of 120W. These process settings were used for all lattices described in this paper.

During initial experimentation, it was observed that lattices whose struts are oriented at an angle of less than roughly 35-40° with respect to the build plane had little or no structural integrity.

Figure 2 illustrates the problem. The default layer thickness with the EBM process is 0.1 mm. At this layer thickness, it is clear that continuity between the layers becomes a problem as the strut angle relative to the built plate decreases. Theoretically speaking, the overlapping distance between adjacent 0.1 mm thick layers can be expressed as L_1-L_2, where L_1=T/sin(α), L_2 = 0.1mm/tan(α), T is the strut thickness, and α is the angle of the strut with the build plane.

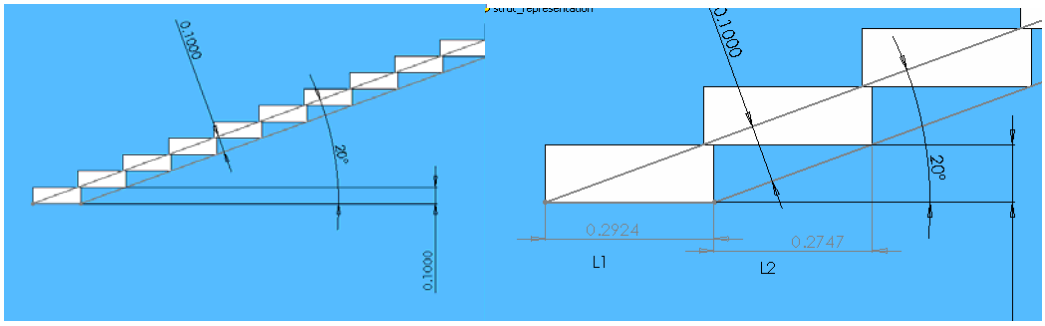

Figure 2 Overlapping Area Between Successive Layers

Figure 3(a) shows a relatively cohesive strut, whereas Figure 3(b) shows a region of relatively poor interlayer bonding resulting from the processing parameters used. These micrographs help to illustrate that the research presented here is very much a starting point, and that further process optimization aimed at improving strut quality is expected to yield improved material properties.

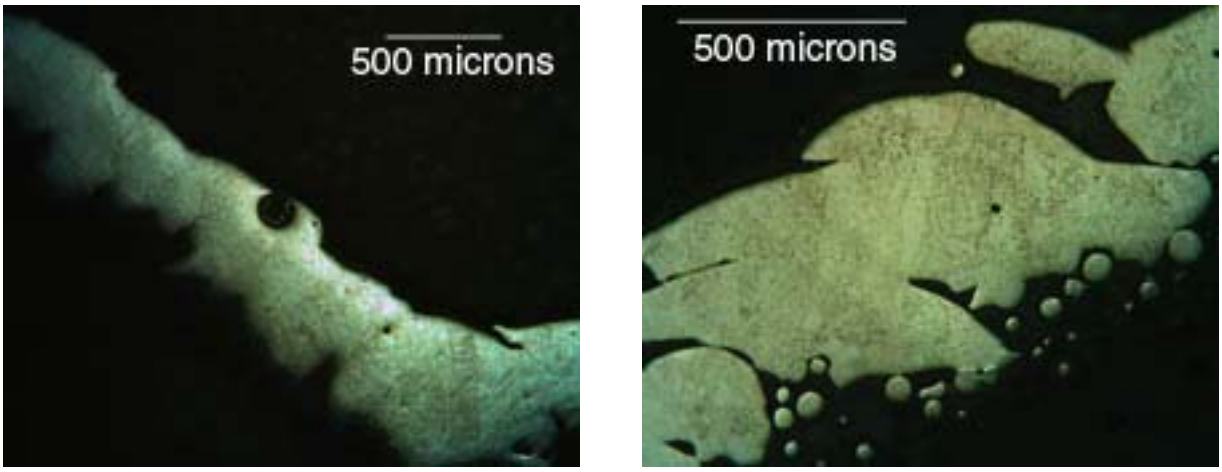

(a) (b)

Figure 3 Range of Strut Qualities

Although numerous different cell geometries have been built, the material properties presented in the remainder of this paper pertain to the hexagonal unit cell that was modeled in Solidworks. Different views of a 3-D array of these unit cells is shown in Figure 4. Unit cells with different overall cell sizes were designed, with each cell having connecting struts of the same 0.7 mm thickness. By maintaining constant beam thickness while increasing or decreasing the cell size, it was possible to compare lattice material properties as a function of overall density. Magics (Materialise) was used to prepare the build files for fabrication on an Arcam EBM S12 (Arcam, Sweden). Slicing of the files was done at 0.1mm layer thickness. The steel start plate was heated up to 750°C before the first layer of powder was melted using the process conditions previously

described. All specimens describe in this paper were built from Ti-6Al-4V powder. Material testing was conducted using an ATS 1605C universal tester. Batches of compression specimens were approximately 25 mm x 25 mm x 25 mm using unit cell dimension of 4 mm, 5 mm, and 6 mm respectively. The specimens were compressed between steel plates at the rate of 5 mm/min. Some samples were also crushed to observe the failure mode. Three-point bending tests were also conducted in same machine using a 50.8 mm span. Length of the bending specimens was approximately 60 mm. The length:thickness ratio was approximately 4 for all bending specimens. The structure modulus and compressive strength were calculated according to the head-displacement reading from compression tests. Specimens were tested in the direction parallel to build direction and also in perpendicular to build direction respectively. These are referred to as the XY and Z orientations respectively.

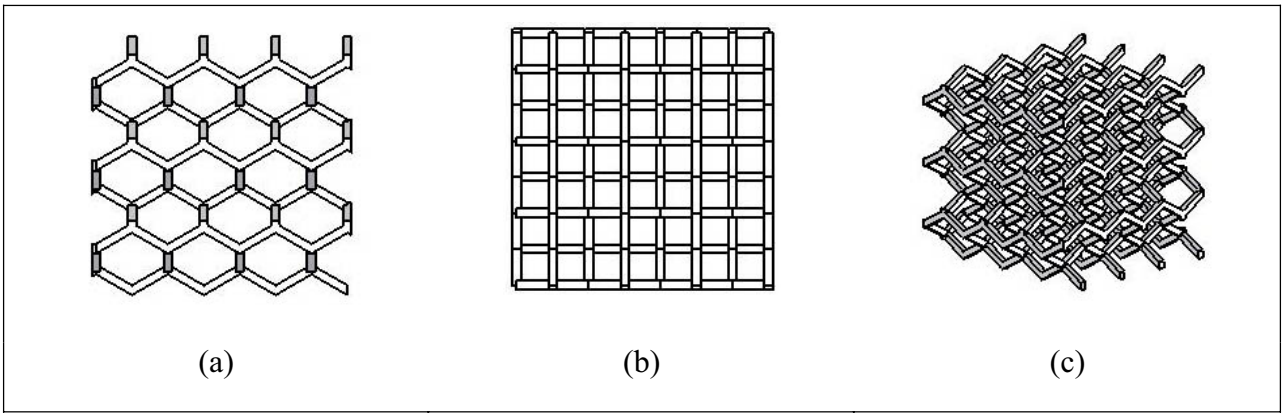

Figure 4 - Top, Front, and Dimetric Views of Hexagonal Lattice Structure

Head displacements were used to calculate the flexural modulus based on the equation

$$E = \frac{(P/y)L^3}{48I}$$

,where E is modulus (MPa), P is load (N), y is deflection (mm), L is loading span (mm), and I is the overall cross sectional moment of inertia (Kg-m^2).

Results and Discussion

Figure 5 shows a variety of non-stochastic cellular structures that were built in a single run on the EBM machine. The same hexagonal cell geometry was used in each case, but replications of structures having 4mm, 5mm, and 6mm unit cell dimensions were built.

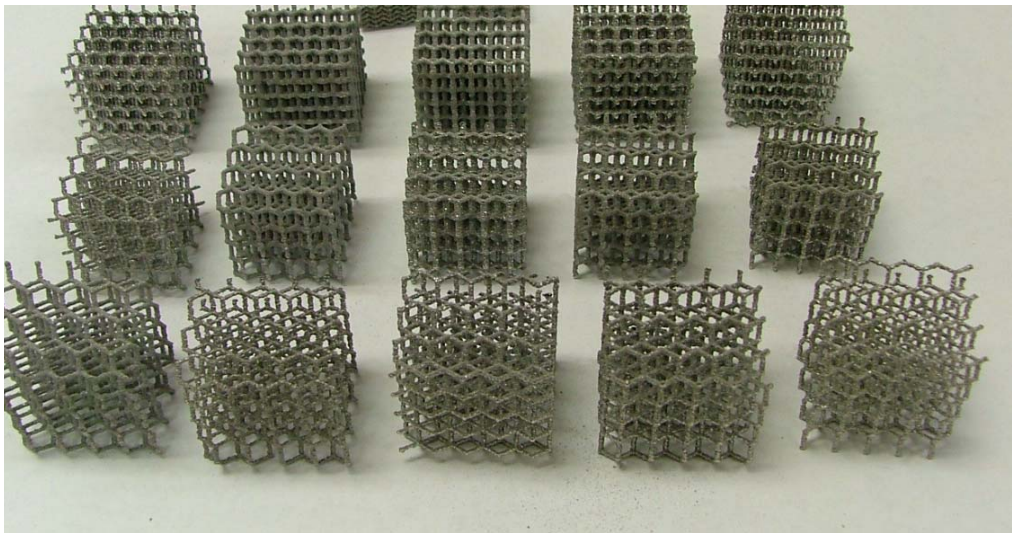

Figure 5 Compression Specimens with 4 mm, 5 mm, and 6 mm Unit Cell Dimensions

Figure 6 shows compression test results for five specimens with 4-mm unit cell dimensions. The XY1, XY2, and XY3 specimens were compressed in a direction parallel to the build direction. The Z1 and Z2 specimens were compressed perpendicular to the build direction. As can be seen from the data, parts loaded parallel to the build direction were stiffer and stronger, but required less work to failure. This trend was also observed for the 5-mm and 6-mm unit cell structures.

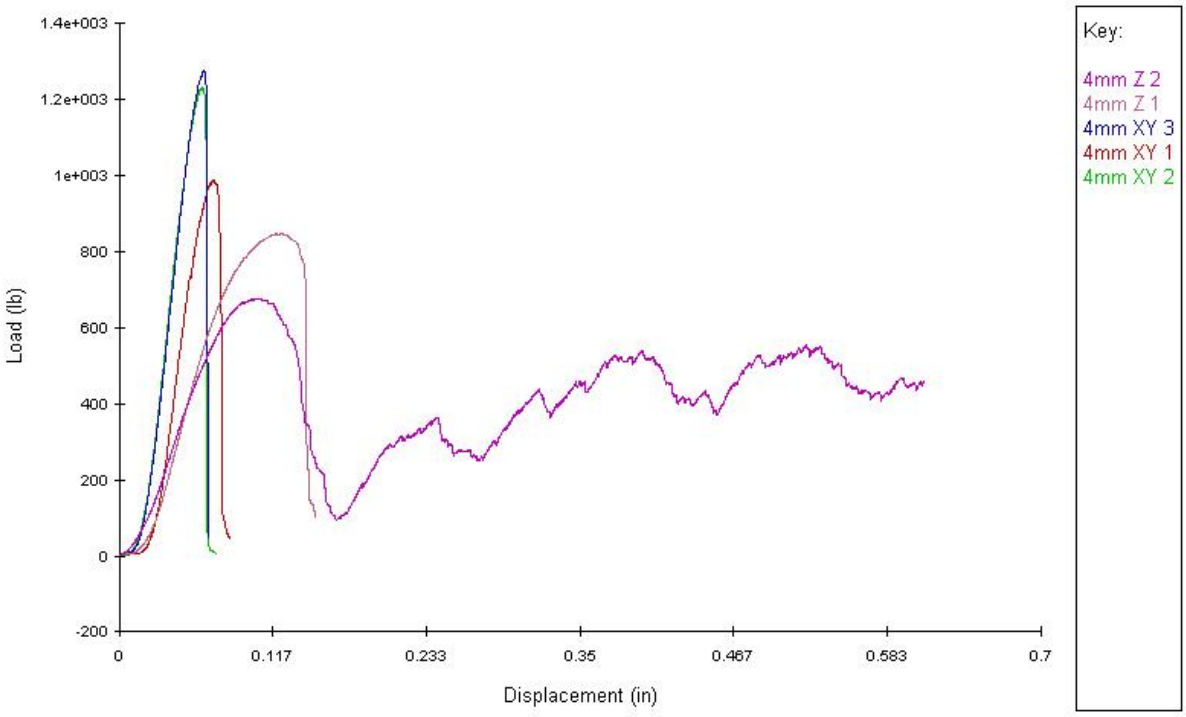

Figure 6 Compression Test Results for 4mm structures

Table 1 summarizes compression test results for the 4-mm structures. Structures built with a 4-mm unit cell dimension have a relative density of less than 11% of solid titanium alloy. The

average measured compressive modulus for specimens loaded parallel to the build direction was 211 MPa.

Specimen	Peak Load (N)	Area (mm^2)	Height (mm)	Compressive strength P/A (MPa)	P/A average (MPa)	Relative density	E_c (MPa)
4mm XY 1	4388.08	597.74	25.5	7.341	**8.78**	0.11	202.403
4mm XY 2	5472.28	585.64	23.7	9.344			211.131
4mm XY 3	5658.57	585.64	23.7	9.662			220.283
4mm Z 1	3754.50	561.69	24.2	6.684	**6.01**		99.275
4mm Z 2	2995.16	561.69	24.2	5.332			79.072

Table 1: 4-mm Structure Compression Test Results

As a means of estimating compressive strength of modulus for structures built with different cell densities, the appropriate formulas from Gibson and Ashby (1988) were consulted. The compressive strength scaling constant was calculated according to the formula

$$\sigma_c = C_1 * \sigma_{c,s} (\frac{p}{p_s})^{1.5}$$

using a solid compressive yield strength of 870 MPa for Ti-6Al-4V. The constant C_1 was set to 0.25 to estimate compressive strength for compression specimens. The standard modulus scaling formula

$$E = C_2 * E_s (\frac{p}{p_s})^2$$

was used with E_s=110 Gpa. The constant C_2 (geometric constants of proportionality) was found to be 0.1656. The modulus and compressive strength results are shown in Figures 7 and 8 with estimations up to 0.2 (i.e. 20%) relative density.

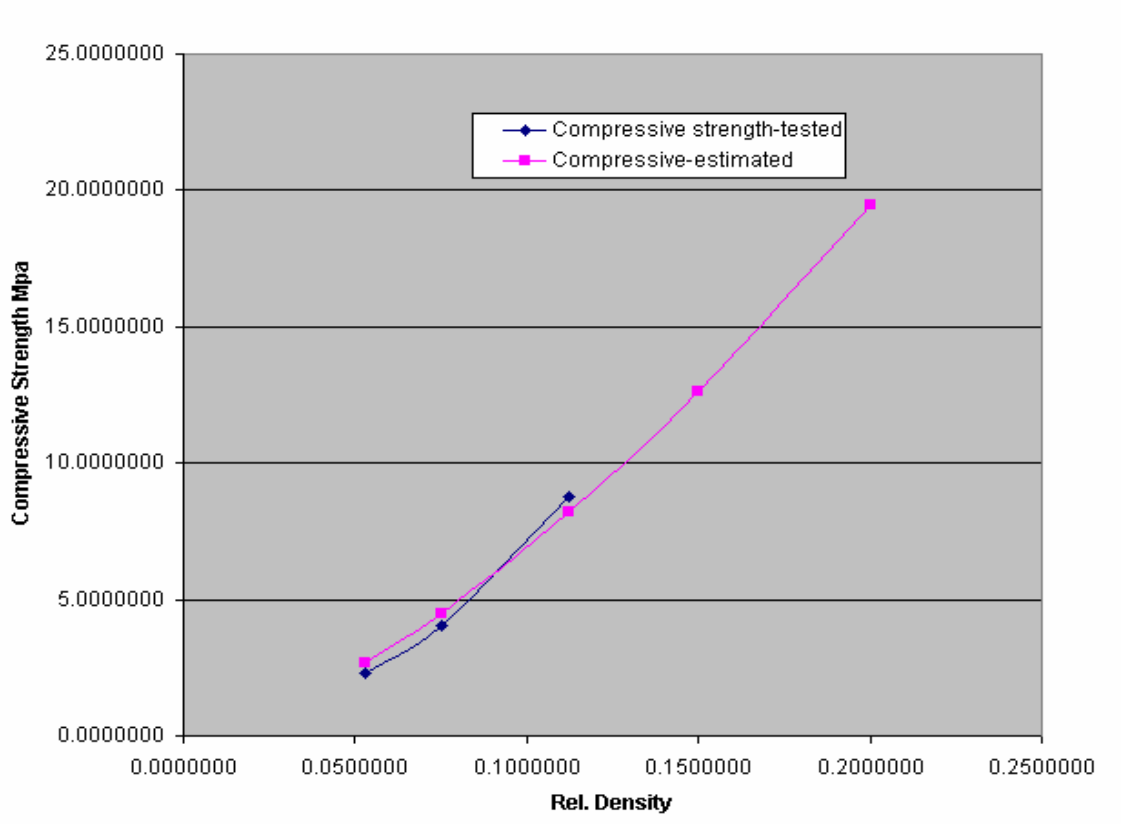

Figure 7 Compressive Strength As a Function of Relative Structure Density

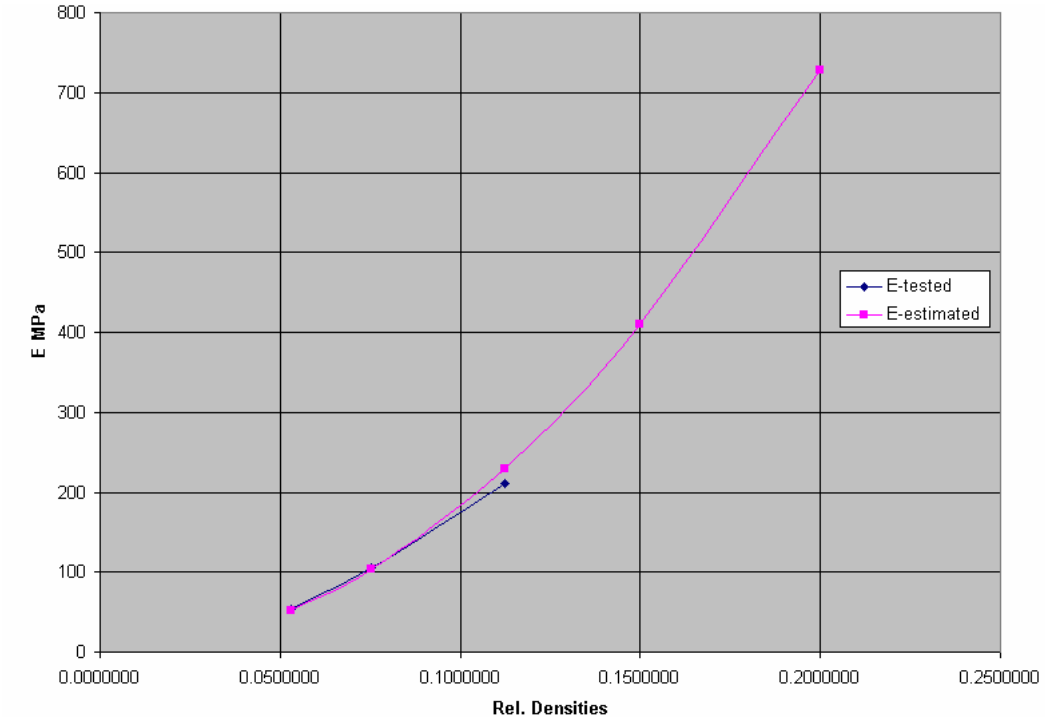

Figure 8 Elastic Modulus as a Function of Relative Structure Density

Following completion of initial compression tests, a set of bars were fabricated for use in 3-point bending tests. A 50.8 mm span was used for all the tests. Loading was done at 0.5 mm/min for all bending specimens. As shown in Figure 9, a subset of the specimens had solid 0.7 mm thick skins built on the top and bottom surfaces. The aim was to increase stiffness and "pin" the ends of the cell struts thus preventing early failure of the meshes. Figure 10 shows the experimental setup.

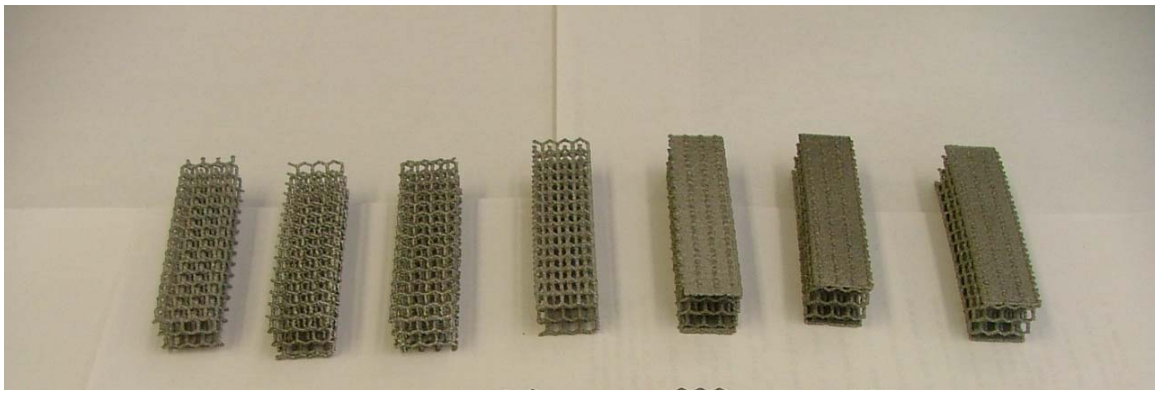

Figure 9 Bending Specimens With and Without Skins

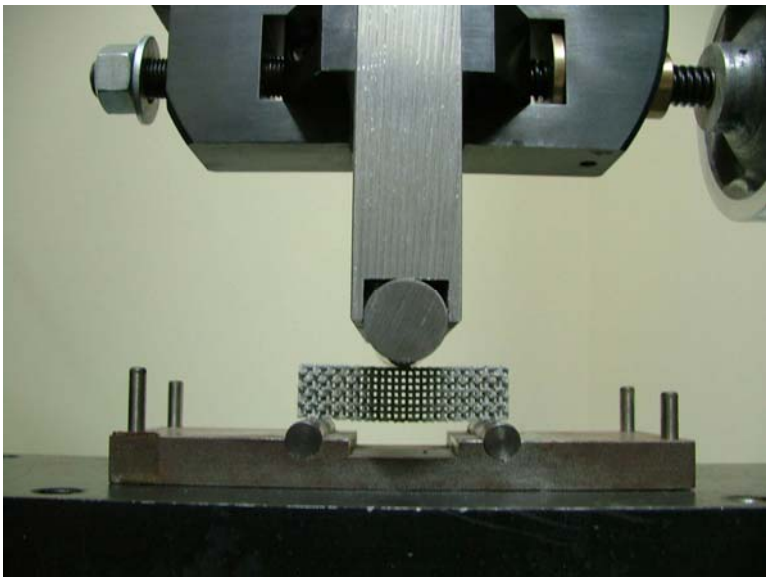

Figure 10 Three Point Bend Test

Figure 11 shows bending test results for the 4-mm structures. Those lines with "skin" in the label had the 0.7 mm thick top/bottom skins, whereas the others did not. It is abundantly clear from the plots that adding a thin skin to the specimens significantly increased stiffness and strength, and extended the plastic region.

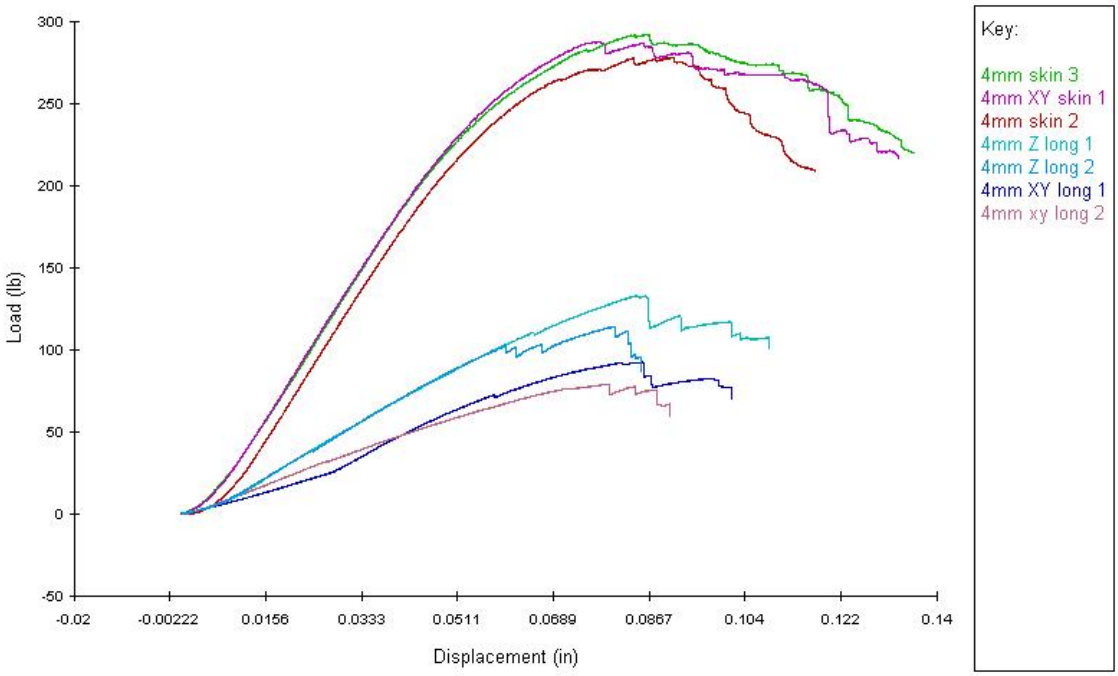

Figure 11 Bending-Load Displacement Plots for 4-mm Structures

For the sake of comparison, a finite element simulation model mimicking the conditions of the bending tests was created in Solidworks cosmos. Figure 12 shows a screen dump from the simulation. The FEA model predicts a compressive modulus of 647.2 MPa. The fact that the predicted modulus is off by approximately a factor of 3 is an important point. Many researchers are developing novel cell geometries and developing simulation models to predict material properties for newly proposed designs. While the models may predict how one design will perform relative to another, the SFF processes do not yet produce struts with perfect cross sections as are those used in idealized models.

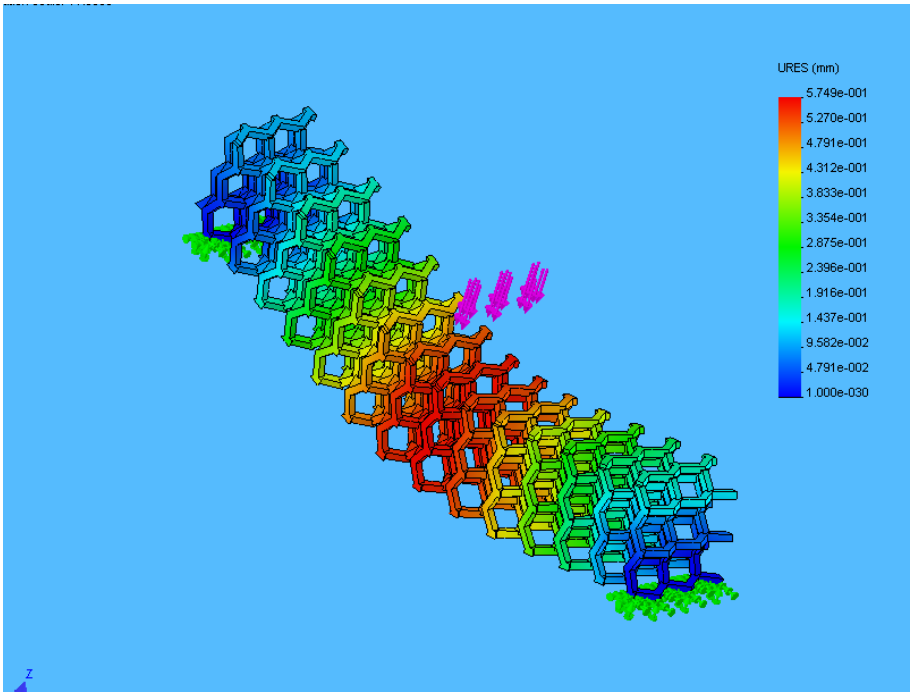

Figure 12 - FEA Model for 4-mm Bending Tests

Conclusions and Future Directions

This paper has reported on preliminary experiments involving the fabrication of titanium alloy non-stochastic lattice structures. It was determined that the smallest strut dimensions that can be fabricated without process optimization is approximately 0.7 mm in diameter. It is furthermore recommended that the strut angle relative to the horizontal build plane not be less than approximately 35° when using 0.7 mm diameter struts. At angles shallower than this, the connectivity between layers is low, and material properties are unacceptable.

A variety of cellular structures have been built in a variety of cell densities ranging from 5% to 11% that of solid Ti-6Al-4V. It was determined that adding solid skins to the tops and bottoms of these structures perpendicular to the expected loading direction dramatically improves material properties.

In terms of future directions, the most obvious need is a more formal process optimization effort to improve strut quality and hence material properties. Part of this study could involve post processing operations such as heat treating to effectively "heal" some of the crack initiation sites.

Many researchers are exploring with different repeating cell geometries. A comprehensive study in which the relative capabilities of each type of geometry are mapped out would be very useful for designers seeking to find suitable cell structures for a given application.

A problem for any of the powder-based (laser and e-beam) SFF approaches is powder removal. Most researchers build structures without skins. However, many real world components require covering with solid skins. Another future topic of study will be to look at the material properties of structures built with solid skins that trap the unmelted powder surrounding the lattice. The

density of the component will still be lower than a solid part due to the fact that the unmelted powder has a lower density. The question to be answered is what the tradeoffs are in strength, stiffness, and weight when a solid skin is built over the part.

References

Banhart, J., (2000) Manufacturing Routes for Metallic Foams. *JOM,* **52,** 22-27.

Baumeister, J., Banhart, J., Weber, M., Aluminium foams for transport industry *Materials & Design,* Vol. 18,4, 217-220, 1997.

Brothers, A. H. and Dunand, D. C. (2006) Amorphous metal foams. *Scripta Materialia,* **54,** 513–520.

Gibson, L. and Ashby, M. (1988) Cellular Solids Structure & Properties, Pergamon Press, NY.

http://www.mcp-group.com/rpt/rpttslm_1.html

Li, J. P., Wijn, J. R., Blitterswijk, C. A. V., and Groot, K., (2006) Porous Ti6Al4V scaffold directly fabricating by rapid prototyping: Preparation and in vitro experiment. *Biomaterials,* **27,** 1223-1235.

Medlin, D. J., Charlebois, S., Swarts, D., Shetty, R., Poggie, R. A., Metallurgical characterization of a porous tantalum biomaterial (Trabecular Metal) for orthopaedic implant applications. Materials & Processes from Medical Devices Conference; Anaheim, CA; USA; 8-10 Sept. 2003. pp. 394-398. 2004

Wadley, H. N.G.; Fleck, N. A.; Evans ,A. G. Fabrication and structural performance of periodic cellular metal sandwich structures. Composites Science and Technology 63 (2003) 2331–2343.

Wen,C.E., Yamada,Y., Shimojima,K., Chino,Y., Hosokawa,H. and Mabuchi,M. (2002) Novel titanium foam for bone tissue engineering. *J. Materia. Res.,* **17,** 2633-2639.

Zhang, X., Ayers, R. A., Thorne, K., Moore, J., and Schowengerdt, F., (2001) Combustion synthesis of porous materials for bone replacement. *Biomed Sci Instrum,* **37,** 463-8.